

Top quark forward-backward asymmetry, FCNC decays and like-sign pair production as a joint probe of new physics

Junjie Cao¹, Lin Wang^{1,2}, Lei Wu², Jin Min Yang²

¹ *College of Physics and Information Engineering,
Henan Normal University, Xinxiang 453007, China*

² *Key Laboratory of Frontiers in Theoretical Physics,
Institute of Theoretical Physics, Academia Sinica, Beijing 100190, China*

Abstract

The anomaly of the top quark forward-backward asymmetry A_{FB}^t observed at the Tevatron can be explained by the t -channel exchange of a neutral gauge boson (Z') which has sizable flavor changing coupling for top and up quarks. This gauge boson can also induce the top quark flavor-changing neutral-current (FCNC) decays and the like-sign top pair production at the LHC. In this work we focus on two models which predict such a Z' , namely the left-right model and the $U(1)_X$ model, to investigate the correlated effects on A_{FB}^t , the FCNC decays $t \rightarrow uV$ ($V = g, Z, \gamma$) and the like-sign top pair production at the LHC. We also pay special attention to the most recently measured A_{FB}^t in the large top pair invariant mass region. We find that under the current experimental constraints both models can alleviate the deviation of A_{FB}^t and, meanwhile, enhance the like-sign top pair production to the detectable level of the LHC. We also find that the two models give different predictions for the observables and their correlations, and thus they may even be distinguished by jointly studying these top quark observables.

PACS numbers: 14.65.Ha, 14.70.Pw, 12.60.Cn

I. INTRODUCTION

In the Standard Model (SM) the top quark is the only fermion with a mass at the electroweak symmetry breaking scale and hence is speculated to be a window on new physics beyond the SM [1]. So far the Tevatron has measured some properties of the top quark and found good agreements with the SM predictions except for the forward-backward asymmetry A_{FB}^t , which shows a 2σ deviation from the SM expectation [2]. Although the latest analysis based on the $5.3fb^{-1}$ luminosity reduced the deviation to about 1.8σ , it indicated that the forward-backward asymmetry depends on the top pair invariant mass $M_{t\bar{t}}$ and for $M_{t\bar{t}} \geq 450$ GeV the deviation is enlarged to 3.4σ [3]. So far various new physics schemes have been proposed to explain such a deviation [4–7], among which one attractive way is the t -channel exchange of a neutral gauge boson Z' which has sizable FCNC coupling for top and up quarks.

These Z' -models are especially interesting because, in addition to contributing to A_{FB}^t , they can also induce the top quark FCNC decays and the like-sign top pair production at the LHC. Due to their suppressed rates in the SM [8] and the rather clean backgrounds [9–12], these FCNC decays and like-sign top pair production can be a good further test of the FCNC Z' models for explanation of A_{FB}^t . On the other hand, the forward-backward asymmetry, the FCNC decays and the like-sign top pair production are correlated with each other and such correlations are model-dependent and thus can help to distinguish different models at the LHC. In this work we concentrate on two such Z' -models, i.e. the left-right model and the $U(1)_X$ model, to study the correlated effects of top quark forward-backward asymmetry at the Tevatron, the FCNC decays $t \rightarrow uV$ ($V = g, Z, \gamma$) and the like-sign top pair production at the LHC.

This work is organized as follows. In Sec. II we briefly describe the two models and present the calculation of the observables. In Sec. III some numerical results are presented. Finally, we draw conclusions in Sec. IV.

II. MODELS AND CALCULATIONS

In extensions of the SM with some extra gauge symmetry, a new neutral gauge boson called Z' is often predicted with family universal or non-universal couplings to fermions.

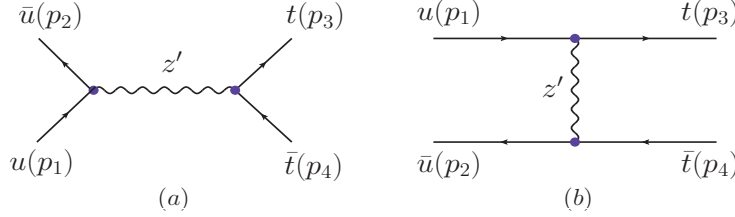


FIG. 1: Feynman diagrams contributing to $t\bar{t}$ production.

For a Z' with family universal couplings, it contributes to the $t\bar{t}$ production only via the s -channel exchange shown in Fig.1(a). Such s -channel contribution does not interfere with the dominant QCD amplitude and thus can not sizably enhance A_{FB}^t . However, the situation is quite different for a Z' with non-universal couplings where the FCNC interaction $Z'\bar{t}_R u_R$ may arise without violating the constraints from flavor physics [6]. In this case, Z' can contribute to $t\bar{t}$ production via the t -channel exchange shown in Fig.1(b), which, as pointed out in [6], can interfere with the QCD amplitude to enhance A_{FB}^t significantly while alter the cross section mildly. Since we attempt to explain the deviation of A_{FB}^t by new physics effects, we in this work consider two models with non-universal Z' couplings, which are called model-I and model-II, respectively.

Model-I extends the SM by a $U(1)_X$ gauge symmetry under which the three generations of the right-handed up-type quarks are charged as $(-1 + \epsilon_U, \epsilon_U, 1 + \epsilon_U)$ [6]. Therefore the new neutral gauge boson Z' predicted in this model only couples to the right-handed quarks, and can safely escape the constraints from Drell-Yan measurement at the Tevatron and LHC[14]. Meanwhile, in this framework, the Yukawa couplings may be generated by the Froggatt-Nielsen type mechanism [15] and the chiral gauge anomalies can be avoided by introducing some extra fermions. The Lagrangian relevant to our discussion is [6]

$$\mathcal{L}_I = g_x \bar{u} \gamma^\mu P_R t Z'_\mu + \sum_{i=1}^3 \epsilon_U g_x \bar{u}_i \gamma^\mu P_R u_i Z'_\mu \quad (1)$$

where g_x and ϵ_U are dimensionless parameters, and i is the generation index. Recently, it is found that this model can explain the deviation of A_{FB}^t and meanwhile satisfy other Tevatron measurements in the parameter region: $120\text{GeV} < m'_Z < 170\text{GeV}$, $\alpha_x = g_x^2/(4\pi) < 0.05$ and $\epsilon_U \leq O(1)$, which is obtained by the following consideration [6]:

- If Z' is heavier than top quark, it will decay dominantly to $t\bar{u}$ or $u\bar{t}$ and consequently give excessive like-sign top quark events through the processes $uu \rightarrow tt$, $ug \rightarrow tZ' \rightarrow t\bar{t}u$ and $u\bar{u} \rightarrow Z'Z' \rightarrow t\bar{u}t\bar{u}$.

- If Z' is much lighter than top quark, the exotic decay $t \rightarrow uZ'$ is open. For $m_{Z'} < 120$ GeV with $\alpha_X = 0.01$, the decay rate will exceed 10%, which can cause a tension between the dileptonic and hadronic channels for the $t\bar{t}$ production at the Tevatron because such a light Z' will decay into light quarks.
- The presence of a small ϵ_U is necessary to make the model phenomenologically viable. If $\epsilon_U = 0$, the only decay mode of Z' is $Z' \rightarrow t\bar{u}$, and then both $u\bar{u} \rightarrow Z'Z'$ and $ug \rightarrow tZ'$ can give the very similar like-sign top pair signal, which is strongly constrained by the Tevatron experiment. A non-zero ϵ_U can avoid this conflict by allowing Z' to decay into $u\bar{u}$. On the other hand, ϵ_U can not be too large because it can enhance the rates of both $p\bar{p} \rightarrow Z' \rightarrow dijet$ and the loop induced decay $t \rightarrow ug$, which have been constrained by the measurements at the Tevatron.

Model-II is a special left-right symmetric model called the third-generation enhanced left-right model, which is based on the gauge group $SU(3)_C \times SU(2)_L \times SU(2)_R \times U(1)_{B-L}$ with gauge couplings g_3 , g_L , g_R and g respectively[16]. The key feature of this model is that the gauge bosons of the $SU(2)_R$ group couple only to the third-generation fermions (the third generation is specially treated) [7, 16]. The gauge interactions relevant to our study are given by

$$\begin{aligned} \mathcal{L}_{II}^Q = & -\frac{g_L}{2\cos\theta_W}\bar{q}\gamma^\mu(g_V - g_A\gamma_5)q(\cos\xi_Z Z_\mu - \sin\xi_Z Z'_\mu) \\ & +\frac{g_Y}{2}\tan\theta_R\left(\frac{1}{3}\bar{q}_L\gamma^\mu q_L + \frac{4}{3}\bar{u}_{Ri}\gamma^\mu u_{Ri} - \frac{2}{3}\bar{d}_{Ri}\gamma^\mu d_{Ri}\right)(\sin\xi_Z Z_\mu + \cos\xi_Z Z'_\mu) \\ & -\frac{g_Y}{2}(\tan\theta_R + \cot\theta_R)(\bar{u}_{Ri}\gamma^\mu V_{Rti}^{u*}V_{Rtj}^u u_{Rj} - \bar{d}_{Ri}\gamma^\mu V_{Rbi}^{d*}V_{Rbj}^d d_{Rj})(\sin\xi_Z Z_\mu + \cos\xi_Z Z'_\mu) \quad (2) \end{aligned}$$

where $\tan\theta_R = g/g_R$, $g_Y = g\cos\theta_R = g_R\sin\theta_R$, ξ_Z is the mixing angle between Z_R and Z_0 , $V_{Rij}^{u,d}$ are the unitary matrices which rotate the right-handed quarks u_{Ri} and d_{Ri} from interaction basis to mass eigenstates and the repeated generation indices i and j are summed. Similar to model-I, a sizable $u_R - t_R$ mixing with other flavor mixings suppressed is allowed by the low energy flavor physics [6]. Such a sizable $u_R - t_R$ mixing can lead to a rather strong $Z'\bar{t}_R u_R$ interaction with the condition $g_R \gg g_Y$.

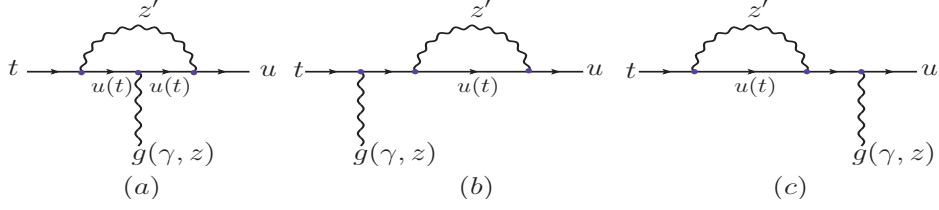


FIG. 2: The loop diagrams contributing to $t \rightarrow uV (V = g, Z, \gamma)$.

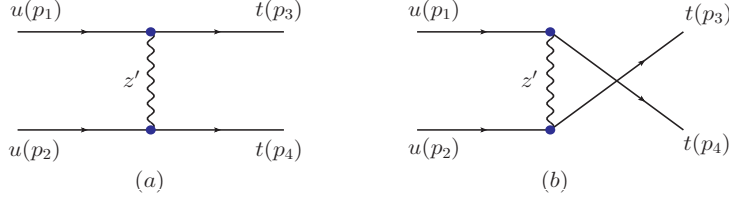


FIG. 3: Feynman diagrams contributing to $t\bar{t}$ production.

Similarly, the interaction to leptons are given as follows[16]:

$$\begin{aligned}
\mathcal{L}_{II}^L = & -\frac{g_L}{2 \cos \theta_W} \bar{\ell} \gamma^\mu (g_V - g_A \gamma_5) \ell (\cos \xi_Z Z_\mu - \sin \xi_Z Z'_\mu) \\
& + \frac{g_Y}{2} \tan \theta_R (-\bar{\ell}_L \gamma^\mu \ell_L - 2 \bar{E}_{Ri} \gamma^\mu E_{Ri}) (\sin \xi_Z Z_\mu + \cos \xi_Z Z'_\mu) \\
& - \frac{g_Y}{2} (\tan \theta_R + \cot \theta_R) (\bar{\nu}_{R\tau} \gamma^\mu \nu_{R\tau} - \bar{\tau}_R \gamma^\mu \tau_R) (\sin \xi_Z Z_\mu + \cos \xi_Z Z'_\mu).
\end{aligned} \tag{3}$$

The constraints on model-II were found [16] to be: $\cot \theta_R \leq 20$ from the requirement of perturbativity, $M_{Z'} \gtrsim 460$ GeV for $\cot \theta_R \geq 10$ from the global fit of the LEP data (especially R_b). Among the oblique parameters, T gives the most stringent constraint, which roughly requires $\xi_Z M_{Z'}/(500\text{GeV}) < 0.01$ at 3σ level. Note that the constraints on $m_{Z'}$ from the CDF search for new resonant states or from the global fitting of the electroweak precision data are not applicable here since they usually assume a Z' with family universal couplings. From the Eqs.(2) and (3), we can see that the flavor-conserving interactions between the dominantly right-handed Z' and the first two generation fermions are suppressed by small $\tan \theta$ for the chosen parameters in our calculation, and thus make a negligible contribution to the process $pp \rightarrow Z' \rightarrow \ell^+ \ell^-$.

Eq.(2) indicates that, unlike model-I, model-II gives an interaction $Z'\bar{t}t$ larger than $Z'\bar{t}u$. Although both models utilize the $Z'\bar{t}u$ interaction to explain the deviation of A_{FB}^t , model-II will have more side effects than model-I, e.g., it may also alter sizably R_b , the total and the differential rates of the $t\bar{t}$ production. The consideration of all these effects leads to a favorable region characterized by a very large g_Y ($10 < \cot \theta_R < 20$) and a heavy Z' ($500\text{GeV} < m_{Z'} < 800\text{GeV}$) [7].

Since both models allow for the FCNC $Z'\bar{t}u$ interaction, they may predict large top quark

FCNC decays $t \rightarrow uV$ ($V = g, Z, \gamma$) and the like-sign top pair production, as shown in Figs.2 and 3. The analytic expressions of the loop amplitudes for the FCNC decays are given in Appendix A. Three points should be noted here. First, in model-I the processes $ug \rightarrow tZ'^* \rightarrow tt\bar{u}$ and $u\bar{u} \rightarrow Z'^*Z'^* \rightarrow t\bar{u}t\bar{u}$ may lead to signals similar to the tt production, which, however, are suppressed by kinematics or high-order effects. Second, in model-II the decay $t \rightarrow uZ$ can proceed at tree level via the $Z - Z'$ mixing, while in model-I it can only occur at loop level. Third, for the signature $ep \rightarrow et$ at the HERA[17], in model I, the lepton-phobic Z' will not contribute to this process and can safely avoid the constraints; For the model II, due to the large Z' mass, the process $ep \rightarrow et$ is less sensitive to the coupling of $Z' u\bar{t}$. Besides, as mentioned above, the small couplings($\tan \theta$) of $Z' e^+e^-$ will cancel the large flavor-changing coupling($\cot \theta$) of $Z' u\bar{t}$ and also not give rise to the significant contribution to process $ep \rightarrow et$.

III. NUMERICAL RESULTS AND DISCUSSIONS

The SM parameters used in this calculations are [18]

$$m_t = 172.5\text{GeV}, m_Z = 91.19\text{ GeV}, \sin^2 \theta_W = 0.2228, \alpha_s(m_t) = 0.1095, \alpha = 1/128. \quad (4)$$

For new physics parameters, we scan them within the following ranges:

$$\text{Model I : } 120\text{ GeV} < m_{Z'} < 170\text{ GeV}, 0.05 < \epsilon_U < 0.1, 0 < \alpha_x < 0.05;$$

$$\text{Model II : } 500\text{ GeV} < m_{Z'} < 2000\text{ GeV}, 10 < \cot \theta < 20, 0.1 < (V_R^u)_{ut} < 0.2, 0 < \xi_Z < 0.01.$$

It should be noted that the contributions to the $t\bar{t}$ cross section mainly come from the flavor-changing t-channel in Fig.1(b) for both models. Since the suppressions of small flavor-conserving coupling ϵ_U in model I and $\tan \theta$ in model II respectively and no interference with the SM QCD process, the s-channel $u\bar{u} \rightarrow Z' \rightarrow t\bar{t}$ has a negligible effects on the $t\bar{t}$ production for both models in our calculations. In additional, the measurements of $t\bar{t}$ cross section at the LHC still have large uncertainties and may not give a new constraints on our two models[19]. In our scan, we require the total cross section of the $t\bar{t}$ production and the differential cross section in each bin of $M_{t\bar{t}}$ to be within the 2σ regions of their experimental values at the Tevatron[20, 21]. For model-II, we also consider the constraint from the T parameter at 3σ level [16]. For the calculation of the hadronic cross sections, we use the parton distribution function CTEQ6L [22] with the renormalization scale μ_R and factorization scale μ_F setting to be m_t .

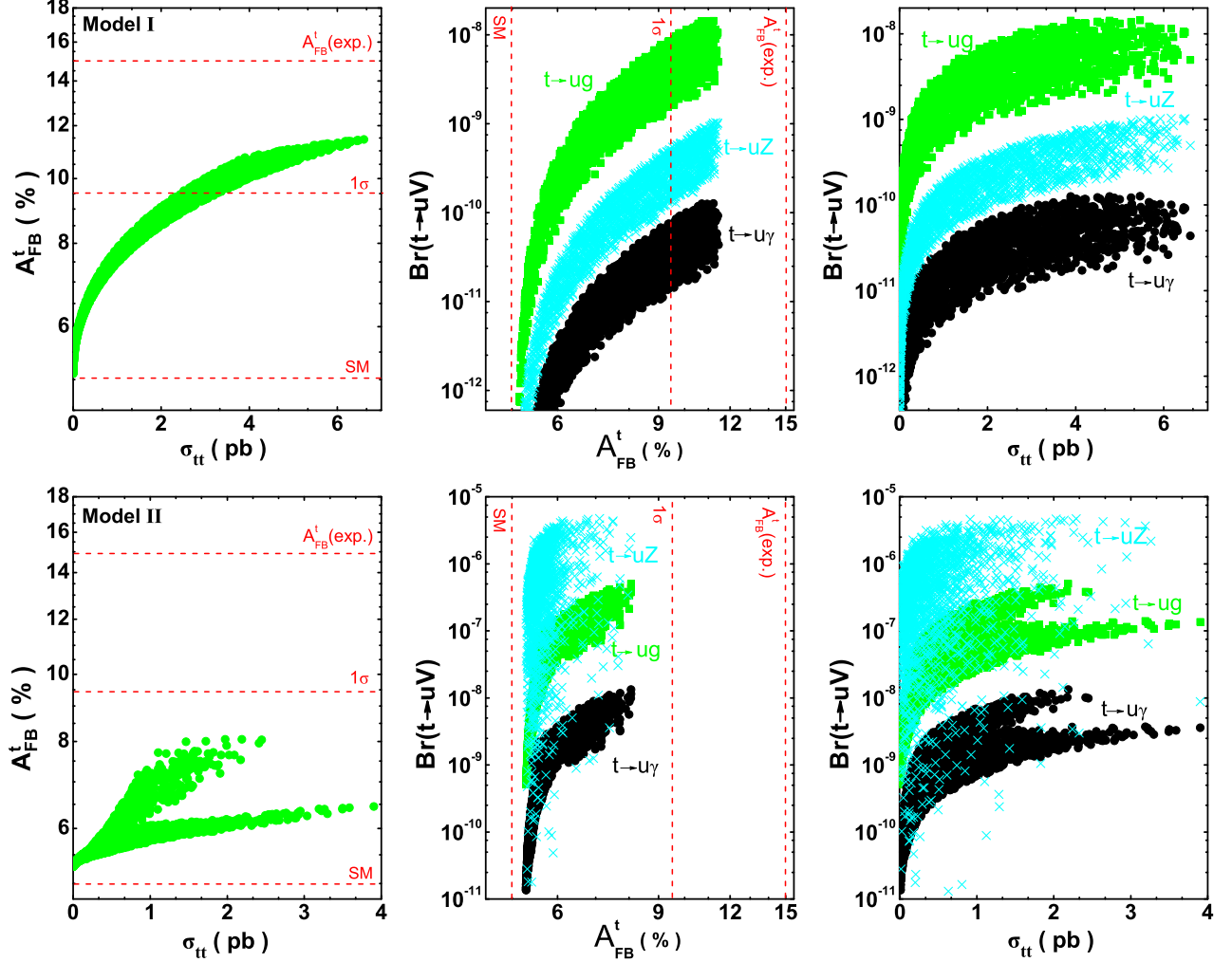


FIG. 4: The correlations between A_{FB}^t at the Tevatron, the branch ratio of top FCNC decays $Br(t \rightarrow uV)$ and the cross section of the tt production $\sigma(tt)$ at the LHC with $\sqrt{s} = 14$ TeV.

A. Correlations between different observables

For each model we show in Fig.4 the correlations between A_{FB}^t at the Tevatron, the branch ratios of the top FCNC decays $Br(t \rightarrow uV)$ and the cross section of the tt production at the LHC with $\sqrt{s} = 14$ TeV. A common feature of the correlations is that all these quantities are proportional to each other. This is obvious since all the quantities receive contributions from the same $Z'\bar{t}u$ interaction. For the forward-backward asymmetry, one can see that both models can enhance its value significantly to alleviate the deviation, especially, model-I can reduce the deviation to 1σ level. More details about the calculation of A_{FB}^t were presented in [7].

About the FCNC decays, Fig.4 shows that $t \rightarrow uZ$ can have a large branching ratio in

model-II because it can proceed at tree level via the $Z - Z'$ mixing. For each decay model-II gives a larger branching ratio than model-I because in model-I the decays are highly suppressed by a factor ϵ_U^2 . Fig.4 also indicates that in both models the branching ratios for these FCNC decays are smaller than 5×10^{-6} , which are far below their current experimental bounds (namely $Br(t \rightarrow ug) < 0.02\%$ from D0 [24], $Br(t \rightarrow u\gamma) < 5.2\%$ from ZEUS¹ [17] and $Br(t \rightarrow uZ) < 3.7\%$ from CDF [25]) and also smaller than the maximal values predicted in other new physics models such as low energy supersymmetry [26], Technicolor model [27] or Little Higgs theory [28]. From the analysis of top FCNC decays [26–29], one can infer that detecting these decays in the present two models would be quite challenging at the LHC.

About the like-sign top pair production, Fig.4 shows that for $A_{FB}^t \geq 6\%$ the cross section in both models can be of pb order, reaching $6.8pb$ in model-I and $3.7pb$ in model-II. Since the signal of such a production is characterized by two isolated like-sign leptons, which is free from the $t\bar{t}$ background and the huge QCD W +jets background [9–11], it may be observable at the LHC and will be discussed in the following.

B. Mass-dependent forward-backward asymmetry at the Tevatron

We note that very recently the CDF reported the dependence of A_{FB}^t on the top pair invariant mass $M_{t\bar{t}}$ and found a more than 3σ discrepancy from the SM prediction for $M_{t\bar{t}} > 450\text{GeV}$ [3]. Motivated by this, we display the dependence of A_{FB}^t on $M_{t\bar{t}}$ in Fig.5. In our calculation, we have included the SM contribution and multiplied the total cross section by a K-factor 1.31 to include the NLO QCD effect [23]. Fig.5 shows that both models can enhance A_{FB}^t in large $M_{t\bar{t}}$ region to ameliorate the discrepancy, though the discrepancy still persists at 2σ level. Further, we note that both models can also cause top quark polarization asymmetry in the $t\bar{t}$ production at the LHC, which was studied recently in [5, 30].

¹ the ZEUS collaboration gives only the upper limits of the anomalous coupling $\kappa_{tu\gamma}$, $\kappa_{t\bar{u}\gamma} < 0.174$ at 95% CL. Using this limits and Eq.(41) in arXiv:hep-ph/0003033 in Ref[1], we can obtain the upper limit $Br(t \rightarrow u\gamma) < 5.2\%$.

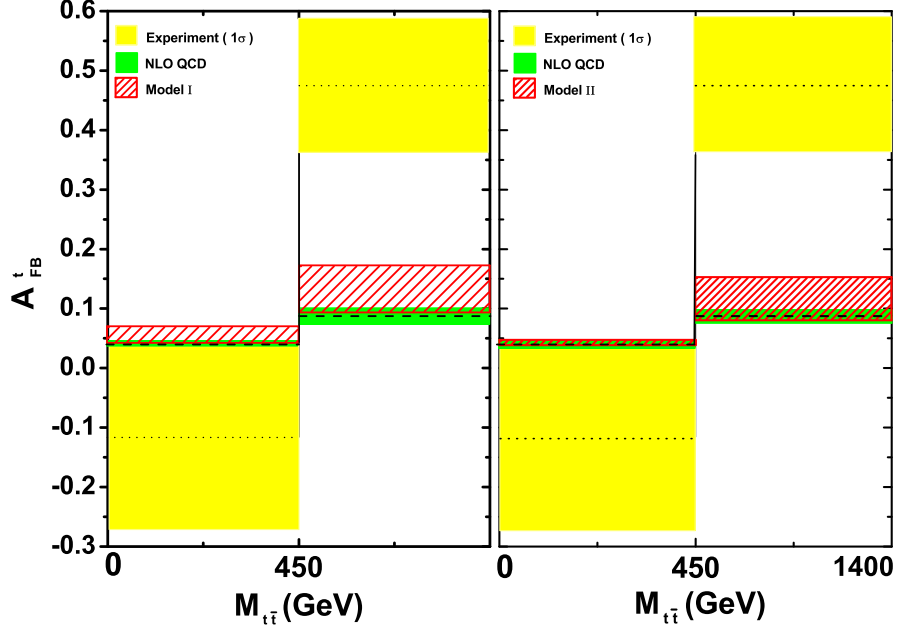


FIG. 5: A_{FB}^t at the Tevatron versus $t\bar{t}$ invariant mass.

C. Like-sign top production at the LHC

Since the like-sign top production can have a large rate and its background is low, we give further study on its observability at the LHC. First, in Fig.6 we display some kinematical distributions such as the top quark transverse momentum p_T^t and its pseudo-rapidity η_t , the total transverse energy H_T of the process and the separation between the two b -jets $\Delta R_{bb} \equiv \sqrt{(\Delta\phi)^2 + (\Delta\eta)^2}$. The new physics parameters are fixed as $\alpha_x = 0.026$ and $m_{Z'} = 170\text{GeV}$ for model-I, and $\cot\theta_R = 20$ and $V_{tu} = 0.2$, $m_{Z'} = 800\text{GeV}$ for model-II. For the last two distributions in Fig.6, we have included the decay chain $t \rightarrow Wb \rightarrow l\nu b$ in our code to simulate the signals of the process. From the upper two and the last frames we can see that the most events are distributed in the region with small transverse momentum or large pseudo-rapidity. This implies that for a light Z' in model-I the top quarks tend to outgo in parallel with the beam pipe. The third frame shows that the two b -jets tend to fly in the opposite direction since they come from the back-to-back top quarks in the $t\bar{t}$ rest frame. The distinct shapes in the second frame are caused by different masses of Z' in the two models (if the Z' mass is assumed to be in the same region for both models, they give the similar shapes).

Now we discuss the detection of the $t\bar{t}$ production at the LHC with $\sqrt{s} = 14\text{TeV}$. We

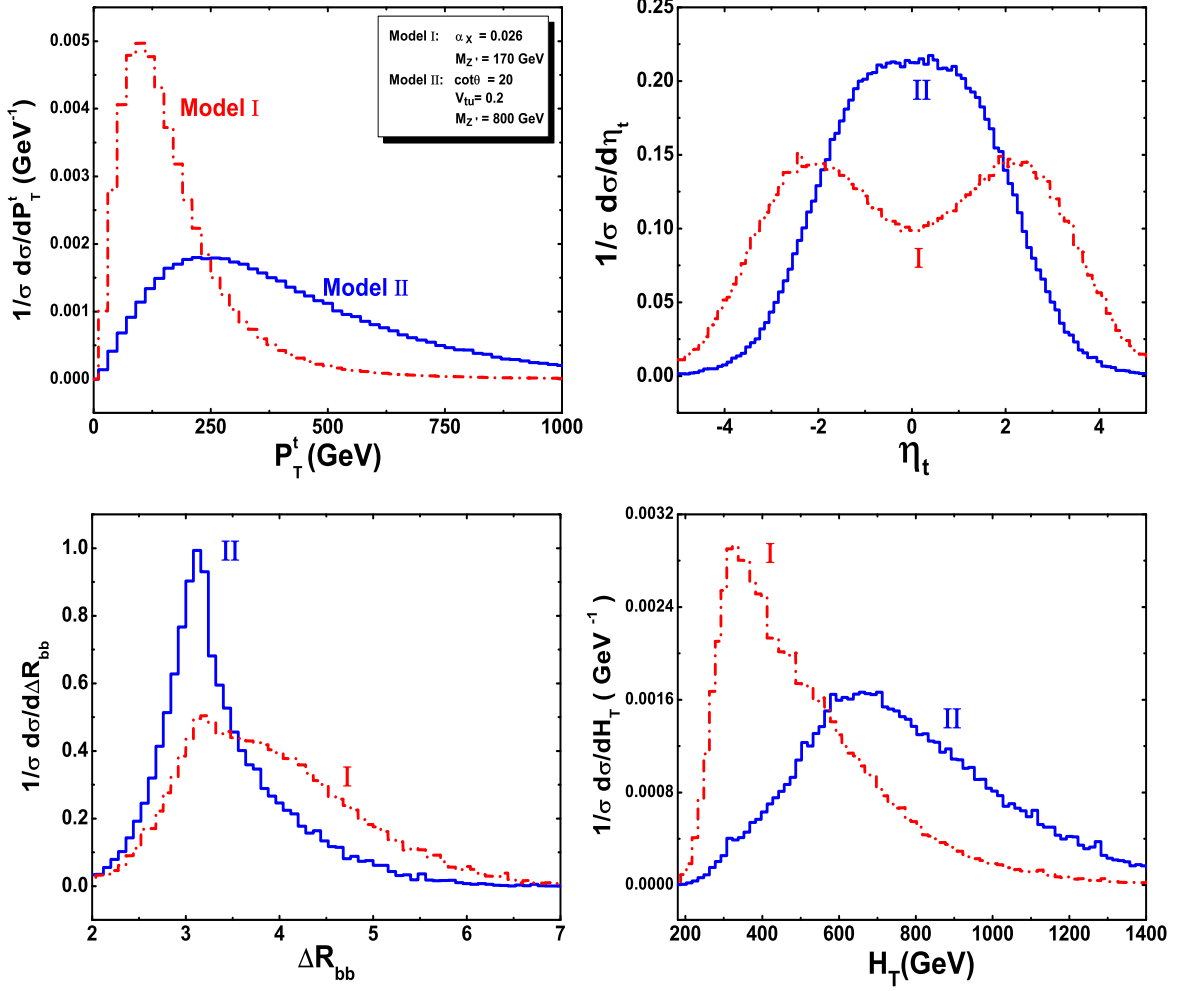


FIG. 6: The p_T^t , η_t , ΔR_{bb} and H_T distributions for the like sign top pair production at the LHC.

choose $\ell_i^+ \ell_j^+ bb \cancel{E}_T$ ($\ell_i = e, \mu$) as the signal. We simulate the energy resolution of the detector effects by assuming a Gaussian smearing for the final leptons and jets [31]

$$\frac{\Delta E}{E} = \frac{5\%}{\sqrt{E}} \oplus 0.55\%, \quad \text{for leptons}, \quad (5)$$

$$\frac{\Delta E}{E} = \frac{100\%}{\sqrt{E}} \oplus 5\% \quad \text{for jets} \quad , \quad (6)$$

where E is in GeV, and \oplus indicates that the energy-dependent and energy-independent terms are added in quadrature. We take the b -jet tagging efficiency as 50%. The main backgrounds are from $qq' \rightarrow t\bar{t}W^\pm$ and $qq \rightarrow W^\pm q' W^\pm q'$, which have been studied in [10]. In our analysis we take the same cuts as in [10] for the signal:

$$\begin{aligned} p_T^\ell &> 15 \text{ GeV}, \quad E_T^j > 40 \text{ GeV}, \quad |\eta_\ell|, |\eta_j| < 2.5, \quad \Delta R_{\ell j}, \Delta R_{jj} > 0.4, \\ M(\ell_1 j_1), M(\ell_2 j_2) &< 160 \text{ GeV}, \quad M(\ell\ell jj) > 500 \text{ GeV}, \end{aligned} \quad (7)$$

TABLE I: 3σ observation bound on the rate of the $t\bar{t}$ production at the LHC with $\sqrt{s} = 14\text{TeV}$ for $100fb^{-1}$ integrated luminosity.

model-I		model-II	
$m_{Z'}$	σ	$m_{Z'}$	σ
120 GeV	27.3 fb	500 GeV	19.7 fb
150 GeV	23.6 fb	1500 GeV	17.8 fb
170 GeV	22.6 fb	2000 GeV	16.5 fb

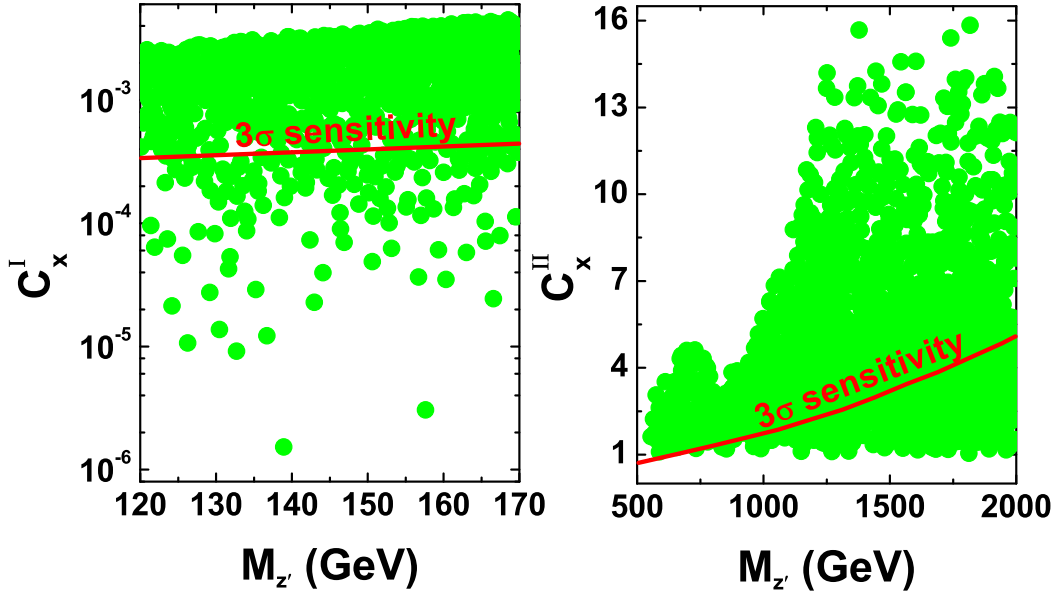


FIG. 7: Surviving samples with C_X^I denoting α_x for model-I and C_X^{II} denoting $V_{tu}^2(\cot\theta + \tan\theta)^2$ for model-II.

where E_T denotes the transverse energy and M is the invariant mass of the final states. Note that the production $pp \rightarrow t\bar{t} \rightarrow bW^+(\rightarrow \ell^+\nu)\bar{b}(\rightarrow \ell^+)W^-(\rightarrow jj)$ can also mimic our signal [12], which, however, has an extra jet and can be suppressed by jet veto.

Under such cuts we find the acceptance rate of the signal is 15.5% for $m_{Z'} = 170\text{GeV}$ in model-I and 18% for $m_{Z'} = 800\text{GeV}$ in model-II. The acceptance rate is found to increase with $m_{Z'}$, which is 12.8% for $m_{Z'} = 120\text{ GeV}$ and increased to 21% for $m_{Z'} = 2000\text{ GeV}$. With the backgrounds calculated in [10], we get the 3σ sensitivity for the $t\bar{t}$ production by requiring $S/\sqrt{S+B} \geq 3$ for $100fb^{-1}$ integrated luminosity. The corresponding results are listed in Table I, where one can learn that the $t\bar{t}$ production with a rate as large as several tens of fb can be detected at the LHC.

Finally, in Fig.7 we project the surviving samples in the scan on the $m_{Z'} - C$ plane with C defined as α_X in model-I and $V_{tu}^2(\cot\theta + \tan\theta)^2$ in model-II. The solid curves in this figure are the 3σ sensitivity and above each curve is the observable region. Our results show that about 83% (88%) of the total surviving samples lie above the 3σ curve for model-I (model-II). Combined with Fig. 4, the points lying below the 3σ curve in Fig.7 give a shift of A_{FB}^t less than 0.5%. This fact implies that if the tt production is not observed at the LHC, then our considered models may not explain the anomaly of A_{FB}^t .

IV. CONCLUSION

In this work we studied the correlations between A_{FB}^t at the Tevatron, the FCNC decays $t \rightarrow uV (V = g, Z, \gamma)$ and the like-sign top pair production at the LHC in two models with non-universal Z' interactions, i.e. the left-right model and the $U(1)_X$ model. We also studied the dependence of A_{FB}^t on the top pair invariant mass $M_{t\bar{t}}$. We found that under the current experimental constraints both models can alleviate the deviation of A_{FB}^t and, meanwhile, enhance the tt production to the detectable level of the LHC. We also found that, since the two models give different predictions for the observables and also their correlations, they may be distinguished by jointly studying these observables. In particular, we emphasize that exploring the tt production at the LHC will allow for a further test of the models which are used to explain the anomaly of A_{FB}^t observed at the Tevatron.

Note Added : Months after our manuscript finished, the CMS collaboration reported their result of searching the like-sign top pair induced by the FCNC Z' at the LHC. The limit of the cross section $\sigma(pp \rightarrow tt(j)) < 17.0$ pb at 95 % CL[32]. We found that in our parameter space, the like-sign top pair cross sections are far bellow the upper limits set by the CMS.

Acknowledgement

This work was supported in part by HASTIT under grant No. 2009HASTIT004, by the National Natural Science Foundation of China (NNSFC) under grant Nos. 10821504, 10725526, 10775039, 11075045 and by the Project of Knowledge Innovation Program (PKIP) of Chinese Academy of Sciences under grant No. KJCX2.YW.W10.

Appendix A: Analytic expressions for FCNC decay amplitudes

Here we list the amplitudes for the loop induced processes $t \rightarrow uV$ ($V = g, \gamma, Z$) shown in Fig.2. The notation $\mathcal{M}(q)$ denotes the amplitude of the diagram with quark q ($q = u, t$) appeared in the loop.

For model-I, the amplitudes are given by

$$\mathcal{M}_g^{(a)}(q) = ag_s T_{\beta\alpha}^A \bar{u}(p_u) [-4C^{\nu\rho} \gamma_\rho - \gamma^\nu + 2B_0^1 \gamma^\nu - 2(\not{p}_t - \not{p}_u) \gamma^\nu \gamma^\rho C_\rho] P_R u(p_t) \varepsilon_\nu^*(p_g), \quad (\text{A1})$$

$$\mathcal{M}_g^{(b)}(q) = ag_s T_{\beta\alpha}^A \bar{u}(p_u) \frac{(2B_1^2 + 1) m_t \not{p}_u \gamma^\nu P_L}{p_u^2 - m_t^2} u(p_t) \varepsilon_\nu^*(p_g), \quad (\text{A2})$$

$$\mathcal{M}_g^{(c)}(q) = ag_s T_{\beta\alpha}^A \bar{u}(p_u) \frac{(2B_1^3 + 1) m_t^2 \gamma^\nu P_R}{p_t^2 - m_u^2} u(p_t) \varepsilon_\nu^*(p_g), \quad (\text{A3})$$

$$\mathcal{M}_\gamma^{(a)}(q) = \frac{2}{3} ea \bar{u}(p_u) [-4C^{\nu\rho} \gamma_\rho - \gamma^\nu + 2B_0^1 \gamma^\nu - 2(\not{p}_t - \not{p}_u) \gamma^\nu \gamma^\rho C_\rho] P_R u(p_t) \varepsilon_\nu^*(p_\gamma), \quad (\text{A4})$$

$$\mathcal{M}_\gamma^{(b)}(q) = \frac{2}{3} ea \bar{u}(p_u) \frac{(2B_1^2 + 1) m_t \not{p}_u \gamma^\nu P_L}{p_u^2 - m_t^2} u(p_t) \varepsilon_\nu^*(p_\gamma), \quad (\text{A5})$$

$$\mathcal{M}_\gamma^{(c)}(q) = \frac{2}{3} ea \bar{u}(p_u) \frac{(2B_1^3 + 1) m_t^2 \gamma^\nu P_R}{p_t^2 - m_u^2} u(p_t) \varepsilon_\nu^*(p_\gamma), \quad (\text{A6})$$

$$\begin{aligned} \mathcal{M}_Z^{(a)}(u) = & -a\delta_{\alpha\beta} g \bar{u}(p_u) \left(\frac{2}{3} \sin \theta_W \tan \theta_W \right) [-4C^{\nu\rho} \gamma_\rho - \gamma^\nu + 2B_0^1 \gamma^\nu \\ & - 2(\not{p}_t - \not{p}_u) \gamma^\nu \gamma^\rho C_\rho] P_R u(p_t) \varepsilon_\nu^*(p_Z), \end{aligned} \quad (\text{A7})$$

$$\begin{aligned} \mathcal{M}_Z^{(a)}(t) = & -a\delta_{\alpha\beta} g \bar{u}(p_u) \left[\frac{m_t^2}{\cos \theta_W} C_0 \gamma^\nu P_R + \frac{2}{3} \sin \theta_W \tan \theta_W [-4C^{\nu\rho} \gamma_\rho \right. \\ & \left. - \gamma^\nu + 2B_0^1 \gamma^\nu - 2(\not{p}_t - \not{p}_u) \gamma^\nu \gamma^\rho C_\rho] P_R \right] u(p_t) \varepsilon_\nu^*(p_Z), \end{aligned} \quad (\text{A8})$$

$$\mathcal{M}_Z^{(b)}(q) = -a\delta_{\alpha\beta} g \bar{u}(p_u) \left(\frac{4 \sin^2 \theta_W - 3}{6 \cos \theta_W} \right) \left[\frac{(2B_1^2 + 1) m_t \not{p}_u \gamma^\nu P_L}{p_u^2 - m_t^2} \right] u(p_t) \varepsilon_\nu^*(p_Z), \quad (\text{A9})$$

$$\mathcal{M}_Z^{(c)}(q) = -a\delta_{\alpha\beta} g \bar{u}(p_u) \left(\frac{2}{3} \sin \theta_W \tan \theta_W \right) \frac{(2B_1^3 + 1) m_t^2 \gamma^\nu P_R}{p_t^2 - m_u^2} u(p_t) \varepsilon_\nu^*(p_Z). \quad (\text{A10})$$

For model-II, the amplitudes are given by

$$\mathcal{M}_g^{(a)}(u) = bg_s T_{\beta\alpha}^A \bar{u}(p_u) [-4C^{\nu\rho} \gamma_\rho - \gamma^\nu + 2B_0^1 \gamma^\nu - 2(\not{p}_t - \not{p}_u) \gamma^\nu \gamma^\rho C_\rho] g_{Z'R}^u P_R u(p_t) \varepsilon_\nu^*(p_g) \quad (\text{A11})$$

$$\begin{aligned} \mathcal{M}_g^{(a)}(t) = & bg_s T_{\beta\alpha}^A \bar{u}(p_u) \{ [-4C^{\nu\rho} \gamma_\rho - \gamma^\nu + 2B_0^1 \gamma^\nu - 2(\not{p}_t - \not{p}_u) \gamma^\nu \gamma^\rho C_\rho] g_{Z'R}^t P_R \\ & + 8m_t C^\nu g_{Z'L}^t P_L - 4m_t (p_u - p_t)^\nu C_0 g_{Z'L}^t P_L \} u(p_t) \varepsilon_\nu^*(p_g), \end{aligned} \quad (\text{A12})$$

$$\mathcal{M}_g^{(b)}(u) = bg_s T_{\beta\alpha}^A \bar{u}(p_u) \frac{(2B_1^2 + 1) m_t \not{p}_u \gamma^\nu g_{Z'R}^u P_L}{p_u^2 - m_t^2} u(p_t) \varepsilon_\nu^*(p_g), \quad (\text{A13})$$

$$\begin{aligned} \mathcal{M}_g^{(b)}(t) = & bg_s T_{\beta\alpha}^A \bar{u}(p_u) \{ (2B_1^2 + 1) m_t \not{p}_u \gamma^\nu g_{Z'R}^t P_L + (4B_0^2 - 2) m_t \not{p}_u \gamma^\nu g_{Z'L}^t P_L \\ & + (4B_0^2 - 2) m_t^2 \gamma^\nu g_{Z'L}^t P_R \} \frac{u(p_t) \varepsilon_\nu^*(p_g)}{p_u^2 - m_t^2}, \end{aligned} \quad (\text{A14})$$

$$\mathcal{M}_g^{(c)}(u) = bg_s T_{\beta\alpha}^A \bar{u}(p_u) \frac{(2B_1^3 + 1)m_t^2 \gamma^\nu g_{Z'R}^u P_R}{p_t^2 - m_u^2} u(p_t) \varepsilon_\nu^*(p_g), \quad (\text{A15})$$

$$\mathcal{M}_g^{(c)}(t) = bg_s T_{\beta\alpha}^A \bar{u}(p_u) \frac{(2B_1^3 + 1)m_t^2 \gamma^\nu g_{Z'R}^t P_R + (4B_0^6 - 2)m_t \gamma^\nu \not{p}_t g_{Z'L}^t P_L}{p_t^2 - m_u^2} u(p_t) \varepsilon_\nu^*(p_g), \quad (\text{A16})$$

$$\mathcal{M}_\gamma^{(a)}(u) = \frac{2}{3} eb \bar{u}(p_u) [-4C^{\nu\rho} \gamma_\rho - \gamma^\nu + 2B_0^1 \gamma^\nu - 2(\not{p}_t - \not{p}_u) \gamma^\nu \gamma^\rho C_\rho] g_{Z'R}^u P_R u(p_t) \varepsilon_\nu^*(p_\gamma), \quad (\text{A17})$$

$$\begin{aligned} \mathcal{M}_\gamma^{(a)}(t) = & \frac{2}{3} eb \bar{u}(p_u) \{ [-4C^{\nu\rho} \gamma_\rho - \gamma^\nu + 2B_0^1 \gamma^\nu - 2(\not{p}_t - \not{p}_u) \gamma^\nu \gamma^\rho C_\rho] g_{Z'R}^t P_R \\ & + 8m_t C^\nu g_{Z'L}^t P_L - 4m_t (p_u - p_t)^\nu C_0 g_{Z'L}^t P_L \} u(p_t) \varepsilon_\nu^*(p_\gamma), \end{aligned} \quad (\text{A18})$$

$$\mathcal{M}_\gamma^{(b)}(u) = \frac{2}{3} eb \bar{u}(p_u) \frac{(2B_1^2 + 1)m_t \not{p}_u \gamma^\nu g_{Z'R}^u P_L}{p_u^2 - m_t^2} u(p_t) \varepsilon_\nu^*(p_\gamma), \quad (\text{A19})$$

$$\begin{aligned} \mathcal{M}_\gamma^{(b)}(t) = & \frac{2}{3} eb \bar{u}(p_u) \{ (2B_1^2 + 1)m_t \not{p}_u \gamma^\nu g_{Z'R}^t P_L + (4B_0^2 - 2)m_t \not{p}_u \gamma^\nu g_{Z'L}^t P_L \\ & + (4B_0^2 - 2)m_t^2 \gamma^\nu g_{Z'L}^t P_R \} \frac{u(p_t) \varepsilon_\nu^*(p_\gamma)}{p_u^2 - m_t^2}, \end{aligned} \quad (\text{A20})$$

$$\mathcal{M}_\gamma^{(c)}(u) = \frac{2}{3} eb \bar{u}(p_u) \frac{(2B_1^3 + 1)m_t^2 \gamma^\nu g_{Z'R}^u P_R}{p_t^2 - m_u^2} u(p_t) \varepsilon_\nu^*(p_\gamma), \quad (\text{A21})$$

$$\mathcal{M}_\gamma^{(c)}(t) = \frac{2}{3} eb \bar{u}(p_u) \frac{(2B_1^3 + 1)m_t^2 \gamma^\nu g_{Z'R}^t P_R + (4B_0^3 - 2)m_t \gamma^\nu \not{p}_t g_{Z'L}^t P_L}{p_t^2 - m_u^2} u(p_t) \varepsilon_\nu^*(p_\gamma). \quad (\text{A22})$$

In above expressions, p_t and p_u denote the momenta of the top and up quark respectively, B and C are loop functions defined in [33] and calculated by LoopTools [34], the dependence of the loop functions on momentums and masses is given by

$$\begin{aligned} B^1(q) &= B(p_t, m_{Z'}, m_q), & B^2(q) &= B(-p_u, m_q, m_{Z'}), \\ B^3(q) &= B(-p_t, m_q, m_{Z'}), & C(q) &= C(-p_u, p_t, m_q, m_{Z'}, m_q), \end{aligned}$$

and the constants are defined by

$$a = -\frac{i}{16\pi^2} \epsilon_\mu g_x^2, \quad (\text{A23})$$

$$b = \frac{i}{16\pi^2} \frac{e^2 V_{Rtu}^{u*} V_{Rtt}^u}{4 \cos^2 \theta_W \sin \theta_W} (\tan \theta_R + \cot \theta_R), \quad (\text{A24})$$

$$g_{Z'L}^{u,t} = (1 - \frac{4}{3} \sin^2 \theta_W) \xi + \frac{1}{3} \sin \theta_W \tan \theta_R, \quad (\text{A25})$$

$$g_{Z'R}^u = -\frac{4}{3} \sin^2 \theta_W \xi + \frac{4}{3} \sin \theta_W \tan \theta_R - \sin \theta_W (\tan \theta_R + \cot \theta_R) V_{Rtu}^{u*} V_{Rtu}^u, \quad (\text{A26})$$

$$g_{Z'R}^t = -\frac{4}{3} \sin^2 \theta_W \xi + \frac{1}{3} \sin \theta_W \tan \theta_R - \sin \theta_W (\tan \theta_R + \cot \theta_R) V_{Rtt}^{u*} V_{Rtt}^u. \quad (\text{A27})$$

[1] For top quark reviews, see, e.g., W. Bernreuther, J. Phys. G **35**, 083001, (2008) D. Chakraborty, J. Konigsberg, D. Rainwater, *Ann. Rev. Nucl. Part. Sci.* **53**, 301 (2003); E. H. Simmons,

- hep-ph/0211335; C.-P. Yuan, hep-ph/0203088; S. Willenbrock, hep-ph/0211067; M. Beneke, *et al.*, hep-ph/0003033; T. Han, arXiv:0804.3178; For model-independent new physics study, see, e.g., C. T. Hill and S. J. Parke, Phys. Rev. D **49**, 4454 (1994); K. Whisnant, *et al.*, Phys. Rev. D **56**, 467 (1997); J. M. Yang, B.-L. Young, Phys. Rev. D **56**, 5907 (1997); K. Hikasa, *et al.*, Phys. Rev. D **58**, 114003 (1998); J. A. Aguilar-Saavedra, arXiv:0811.3842; R.A. Coimbra, *et al.*, arXiv:0811.1743.
- [2] G. Stricker *et al.*, CDF note 9724 (2009); T. Aaltonen *et al.* [CDF Collaboration], Phys. Rev. Lett. 101, 202001 (2008); V. M. Abazov *et al.* [D0 Collaboration], Phys. Rev. Lett. 100, 142002 (2008).
- [3] T. Aaltonen *et al.* [The CDF Collaboration], arXiv:1101.0034 [hep-ex].
- [4] A. Djouadi *et al.*, Phys. Rev. D **82**, 071702 (2010); P. Ferrario, G. Rodrigo, Phys. Rev. D **80**, 051701 (2009); K. Cheung, W. Y. Keung, T. C. Yuan, Phys. Lett. B **682**, 287 (2009); S. Jung *et al.*, Phys. Rev. D **81**, 015004 (2010); J. Shu, T. Tait, K. Wang, Phys. Rev. D **81**, 034012 (2010); P. H. Frampton, J. Shu, K. Wang, Phys. Rev. D **683**, 294 (2010); A. Arhrib, R. Benbrik, C. H. Chen, Phys. Rev. D **82**, 034034 (2010); I. Dorsner *et al.*, Phys. Rev. D **81**, 055009 (2010); D. W. Jung *et al.*, Phys. Lett. B **691**, 238 (2010); V. Ahrens *et al.*, JHEP **1009**, 097 (2010); M. V. Martynov, A. D. Smirnov, Mod. Phys. Lett. A **25**, 2637 (2010); R. S. Chivukula, E. H. Simmons, C.-P. Yuan, Phys. Rev. D **82**, 094009 (2010); Q.-H. Cao *et al.*, Phys. Rev. D **81**, 114004 (2010); G. Rodrigo and P. Ferrario, arXiv:1007.4328; V. Barger, W.-Y. Keung, C.-T. Yu, Phys. Rev. D **81**, 113009 (2010); M. Bauer *et al.*, JHEP 1011, 039 (2010); C. Zhang, S. Willenbrock, arXiv:1008.3869; J. A. Aguilar-Saavedra, Nucl. Phys. B **843**, 638 (2011); C. H. Chen, G. Cvetič, C. S. Kim, arXiv:1009.4165; K. Kumar *et al.*, JHEP 1008, 052 (2010); C. Degrande *et al.*, arXiv:1010.6304 [hep-ph]; B. Xiao, Y.-K. Wang, S. h. Zhu, Phys. Rev. D **82**, 034026 (2010); arXiv:1011.0152; arXiv:1101.2507; G. Burdman, L. Lima, R. D. Matheus, arXiv:1011.6380; E. Alvarez, L. Rold, A. Szyrkman, arXiv:1011.6557; D. W. Jung *et al.*, arXiv:1012.0102; K. Cheung, T. C. Yuan, arXiv:1101.1445; C. Delaunay *et al.*, arXiv:1101.2902.
- [5] D. W. Jung, P. Ko and J. S. Lee, arXiv:1011.5976; D. Choudhury *et al.*, arXiv:1012.4750.
- [6] S. Jung, H. Murayama, A. Pierce and J. D. Wells, Phys. Rev. D **81**, 015004 (2010).
- [7] J. Cao *et al.*, Phys. Rev. D **81**, 014016 (2010);
- [8] See for example, G. Eilam, J. L. Hewett and A. Soni, Phys. Rev. D **44**, 1473 (1991); B. Mele,

- S. Petrarca and A. Soddu, Phys. Lett. B **435**, 401 (1998).
- [9] T. Stelzer, Z. Sullivan and S. Willenbrock, Phys. Rev. D **58**, 094021 (1998); W. S. Hou *et al.*, Phys. Lett. B **409**, 344 (1997); F. Larios and F. Penunuri, J. Phys. G **30**, 895 (2004); J. Cao *et al.*, Phys. Rev. D **70**, 114035 (2004); O. Cakir *et al.*, Eur. Phys. J. C **70**, 295 (2010); O. Gedalia, L. Mannelli and G. Perez, JHEP **1010**, 046 (2010).
- [10] Yu. P. Gouz and S. R. Slabospitsky, Phys. Lett. B **457**, 177 (1999).
- [11] S. K. Gupta, arXiv:1011.4960 [hep-ph].
- [12] E. L. Berger, Q. H. Cao, C. R. Chen, G. Shaughnessy and H. Zhang, Phys. Rev. Lett. **105**, 181802 (2010) H. Zhang, E. L. Berger, Q. H. Cao, C. R. Chen and G. Shaughnessy, Phys. Lett. B **696**, 68 (2011)
- [13] T. Aaltonen *et al.* [CDF Collaboration], Phys. Rev. Lett. **102**, 041801 (2009);
- [14] M. S. Carena, A. Daleo, B. A. Dobrescu and T. M. P. Tait, Phys. Rev. D **70**, 093009 (2004) [arXiv:hep-ph/0408098]. T. Aaltonen *et al.* [The CDF Collaboration], Phys. Rev. Lett. **106**, 121801 (2011) [arXiv:1101.4578 [hep-ex]]. S. Chatrchyan *et al.* [CMS Collaboration], JHEP **1105**, 093 (2011) [arXiv:1103.0981 [hep-ex]].
- [15] C. D. Froggatt and H. B. Nielsen, Nucl. Phys. B **147**, 277 (1979).
- [16] X. G. He and G. Valencia, Phys. Rev. D **66**, 013004 (2002); Phys. Rev. D **68**, 033011 (2003).
- [17] S. Chekanov *et al.* [ZEUS Collaboration], Phys. Lett. B **559**, 153 (2003).
- [18] C. Amsler *et al.*, Particle Data Group, Phys. Lett. B **667**, 1 (2008).
- [19] <http://cdsweb.cern.ch/record/1336491/files/TOP-11-001-pas.pdf>
- [20] T. Aaltonen *et al.* [The CDF Collaboration], Phys. Rev. D **82**, 052002 (2010);
- [21] T. Aaltonen *et al.* [CDF Collaboration], Phys. Rev. Lett. **102**, 222003 (2009).
- [22] J. Pumplin *et al.*, JHEP **0602**, 032 (2006).
- [23] M. Cacciari *et al.*, JHEP **0809**, 127 (2008); S. Moch and P. Uwer, Phys. Rev. D **78**, 034003 (2008); N. Kidonakis and R. Vogt, Phys. Rev. D **78**, 074005 (2008);
- [24] V. M. Abazov *et al.* [D0 Collaboration], Phys. Lett. B **693**, 81 (2010).
- [25] T. Aaltonen *et al.* [CDF Collaboration], Phys. Rev. Lett. **101**, 192002 (2008).
- [26] See, e.g., C. S. Li, R. J. Oakes, J. M. Yang, Phys. Rev. D **49**, 293 (1994); G. Couture, C. Hamzaoui, H. Konig, Phys. Rev. D **52**, 1713 (1995); J. L. Lopez, D. V. Nanopoulos, R. Rangarajan, Phys. Rev. D **56**, 3100 (1997); J. M. Yang, B. L. Young, X. Zhang, Phys. Rev. D **58**, 055001 (1998); J. M. Yang, C. S. Li, Phys. Rev. D **49**, 3412 (1994); J. Guasch,

- J. Sola, Nucl. Phys. B **562**, 3 (1999); G. Eilam *et al.*, Phys. Lett. B **510**, 227 (2001); C. S. Li, L. Yang, L. Jin, Phys. Lett. B **599**, 92 (2004); Z. Heng *et al.*, Phys. Rev. D **79**, 094029 (2009); J. Cao *et al.*, Phys. Rev. D **79**, 054003 (2009); Phys. Rev. D **75**, 075021 (2007); Phys. Rev. D **74**, 031701 (2006); Nucl. Phys. B **651**, 87 (2003).
- [27] X. Wang *et al.*, Phys. Rev. D **50**, 5781 (1994); G. Lu *et al.*, Phys. Rev. D **68**, 015002 (2003); J. Cao *et al.*, Phys. Rev. D **76**, 014004 (2007); Phys. Rev. D **67**, 071701 (2003); H. J. Zhang, Phys. Rev. D **77**, 057501 (2008).
- [28] X.-F. Han, L. Wang, J. M. Yang, arXiv:0903.5491; X. Wang, *et al.*, Nucl. Phys. B **807**, 210 (2009); Y. Zhang, G. Lu, X. Wang, arXiv:1011.0552;
- [29] J. J. Zhang, *et al.*, Phys. Rev. Lett. **102**, 072001 (2009); J. Drobnak, S. Fajfer and J. F. Kamenik, Phys. Rev. Lett. **104**, 252001 (2010); Phys. Rev. D **82**, 073016 (2010).
- [30] J. Cao, L. Wu, J. M. Yang, arXiv:1011.5564 [hep-ph].
- [31] G. Aad *et al.* [The ATLAS Collaboration], arXiv:0901.0512 [hep-ex].
- [32] S. Chatrchyan *et al.* [CMS Collaboration], arXiv:1106.2142 [hep-ex].
- [33] B. A. Kniehl, Phys. Rep. **240**, 211 (1994).
- [34] T. Hahn, M. Perez-Victoria, Comput. Phys. Commun. **118**, 153 (1999); T. Hahn, Nucl. Phys. Proc. Suppl. **135**, 333 (2004).